Femtosecond laser-assisted synthesis of highly photoluminescent carbon nanodots for Fe^{3+} detection with high sensitivity and selectivity

Vanthan Nguyen,[1,2] Lihe Yan,[1,*] Jinhai Si,[1] and Xun Hou[1]

[1]*Key Laboratory for Physical Electronics and Devices of the Ministry of Education and Shaanxi Key Lab of Information Photonic Technique, School of Electronics and Information Engineering, Xi'an Jiaotong University, Xi'an 710049, China*

[2]*Le Quy Don Technical University, Hanoi 122314, Vietnam*

[*]*liheyan@mail.xjtu.edu.cn*

Abstract: Carbon nanodots (C-dots) were synthesized by femtosecond laser ablation of graphite powders in polyethylene glycol (PEG_{200N}) solutions with different graphite concentrations. The photoluminescent quantum yield (PLQY) of the C-dots was effectively enhanced by decreasing the graphite concentration, and its value could reach 21%. Detailed work showed that the C-dots prepared with a low raw material concentration possessed high PLQY because they contained fewer trap defects in the carbogenic core and a larger quantity of surface functional groups on the surface. Taking advantage of their high photoluminescence properties, the C-dots were used as effective fluorescent nanosensor probes for sensitive and selective detection of Fe^{3+} ions.

©2016 Optical Society of America

OCIS codes: (160.4236) Nanomaterials; (160.2540) Fluorescent and luminescent materials.

References and links

1. P. D. Howes, R. Chandrawati, and M. M. Stevens, "Colloidal nanoparticles as advanced biological sensors," Science **346**(6205), 1247390 (2014).
2. H. Li, Z. Kang, Y. Liu, and S.-T. Lee, "Carbon nanodots: synthesis, properties and applications," J. Mater. Chem. **22**(46), 24230 (2012).
3. K. Hola, Y. Zhang, Y. Wang, E. P. Giannelis, R. Zboril, and A. L. Rogach, "Carbon dots-Emerging light emitters for bioimaging, cancer therapy and optoelectronics," Nano Today **9**(5), 590–603 (2014).
4. J. Wang, F. Peng, Y. Lu, Y. Zhong, S. Wang, M. Xu, X. Ji, Y. Su, L. Liao, and Y. He, "Large-scale green synthesis of fluorescent carbon nanodots and their use in optics applications," Adv. Opt. Mater. **3**(1), 103–111 (2015).
5. H. Nie, M. Li, Q. Li, S. Liang, Y. Tan, L. Sheng, W. Shi, and S. X.-A. Zhang, "Carbon dots with continuously tunable full-color emission and their application in ratiometric pH sensing," Chem. Mater. **26**(10), 3104–3112 (2014).
6. S. T. Yang, L. Cao, P. G. Luo, F. Lu, X. Wang, H. Wang, M. J. Meziani, Y. Liu, G. Qi, and Y. P. Sun, "Carbon dots for optical imaging in vivo," J. Am. Chem. Soc. **131**(32), 11308–11309 (2009).
7. J. Tang, B. Kong, H. Wu, M. Xu, Y. Wang, Y. Wang, D. Zhao, and G. Zheng, "Carbon nanodots featuring efficient FRET for real-time monitoring of drug delivery and two-photon imaging," Adv. Mater. **25**(45), 6569–6574 (2013).
8. W. F. Zhang, H. Zhu, S. F. Yu, and H. Y. Yang, "Observation of lasing emission from carbon nanodots in organic solvents," Adv. Mater. **24**(17), 2263–2267 (2012).
9. X. Zhang, Y. Zhang, Y. Wang, S. Kalytchuk, S. V. Kershaw, Y. Wang, P. Wang, T. Zhang, Y. Zhao, H. Zhang, T. Cui, Y. Wang, J. Zhao, W. W. Yu, and A. L. Rogach, "Color-switchable electroluminescence of carbon dot light-emitting diodes," ACS Nano **7**(12), 11234–11241 (2013).
10. S. K. Sahoo, D. Sharma, R. K. Bera, G. Crisponi, and J. F. Callan, "Iron(III) selective molecular and supramolecular fluorescent probes," Chem. Soc. Rev. **41**(21), 7195–7227 (2012).
11. S. Zhu, Q. Meng, L. Wang, J. Zhang, Y. Song, H. Jin, K. Zhang, H. Sun, H. Wang, and B. Yang, "Highly photoluminescent carbon dots for multicolor patterning, sensors, and bioimaging," Angew. Chem. Int. Ed. **52**(14), 3953–3957 (2013).
12. Z. S. Qian, L. J. Chai, Y. Y. Huang, C. Tang, J. J. Shen, J. R. Chen, and H. Feng, "A real-time fluorescent assay for the detection of alkaline phosphatase activity based on carbon quantum dots," Biosens. Bioelectron. **68**, 675–680 (2015).

#253046 Received 2 Nov 2015; revised 20 Dec 2015; accepted 21 Dec 2015; published 5 Jan 2016
© 2016 OSA

13. J. Zong, X. Yang, A. Trinchi, S. Hardin, I. Cole, Y. Zhu, C. Li, T. Muster, and G. Wei, "Carbon dots as fluorescent probes for "off-on" detection of Cu^{2+} and L-cysteine in aqueous solution," Biosens. Bioelectron. **51**, 330–335 (2014).
14. S.-L. Hu, K.-Y. Niu, J. Sun, J. Yang, N.-Q. Zhao, and X.-W. Du, "One-step synthesis of fluorescent carbon nanoparticles by laser irradiation," J. Mater. Chem. **19**(4), 484–488 (2009).
15. K. Habiba, V. I. Makarov, J. Avalos, M. J. F. Guinel, B. R. Weiner, and G. Morell, "Luminescent graphene quantum dots fabricated by pulsed laser synthesis," Carbon **64**, 341–350 (2013).
16. D. Werner, A. Furube, T. Okamoto, and S. Hashimoto, "Femtosecond laser-induced size reduction of aqueous gold nanoparticles: In situ and pump–probe spectroscopy investigations revealing Coulomb explosion," J. Phys. Chem. C **115**(17), 8503–8512 (2011).
17. V. Amendola and M. Meneghetti, "What controls the composition and the structure of nanomaterials generated by laser ablation in liquid solution?" Phys. Chem. Chem. Phys. **15**(9), 3027–3046 (2013).
18. D. Tan, S. Zhou, J. Qiu, and N. Khusro, "Preparation of functional nanomaterials with femtosecond laser ablation in solution," J. Photochem. Photobiol. Chem. **17**, 50–68 (2013).
19. D. Tan, S. Zhou, B. Xu, P. Chen, Y. Shimotsuma, K. Miura, and J. Qiu, "Simple synthesis of ultra-small nanodiamonds with tunable size and photoluminescence," Carbon **62**, 374–381 (2013).
20. D. Tan, G. Lin, Y. Liu, Y. Teng, Y. Zhuang, B. Zhu, Q. Zhao, and J. Qiu, "Synthesis of nanocrystalline cubic zirconia using femtosecond laser ablation," J. Nanopart. Res. **13**(3), 1183–1190 (2011).
21. V. Nguyen, L. Yan, J. Si, and X. Hou, "Femtosecond laser-induced size reduction of carbon nanodots in solution: Effect of laser fluence, spot size, and irradiation time," J. Appl. Phys. **117**(8), 084304 (2015).
22. V. Nguyen, J. Si, L. Yan, and X. Hou, "Electron–hole recombination dynamics in carbon nanodots," Carbon **95**, 659–663 (2015).
23. Z.-Q. Xu, L.-Y. Yang, X.-Y. Fan, J.-C. Jin, J. Mei, W. Peng, F.-L. Jiang, Q. Xiao, and Y. Liu, "Low temperature synthesis of highly stable phosphate functionalized two color carbon nanodots and their application in cell imaging," Carbon **66**, 351–360 (2014).
24. P. Blandin, K. A. Maximova, M. B. Gongalsky, J. F. Sanchez-Royo, V. S. Chirvony, M. Sentis, V. Y. Timoshenko, and A. V. Kabashin, "Femtosecond laser fragmentation from water-dispersed microcolloids: toward fast controllable growth of ultrapure Si-based nanomaterials for biological applications," J. Mater. Chem. B **1**(19), 2489 (2013).
25. L. Tang, R. Ji, X. Cao, J. Lin, H. Jiang, X. Li, K. S. Teng, C. M. Luk, S. Zeng, J. Hao, and S. P. Lau, "Deep ultraviolet photoluminescence of water-soluble self-passivated graphene quantum dots," ACS Nano **6**(6), 5102–5110 (2012).
26. S. A. Kulinich, T. Kondo, Y. Shimizu, and T. Ito, "Pressure effect on ZnO nanoparticles prepared via laser ablation in water," J. Appl. Phys. **113**(3), 033509 (2013).
27. T. Tsuji, D. H. Thang, Y. Okazaki, M. Nakanishi, Y. Tsuboi, and M. Tsuji, "Preparation of silver nanoparticles by laser ablation in polyvinylpyrrolidone solutions," Appl. Surf. Sci. **254**(16), 5224–5230 (2008).
28. Y. Feng, J. Zhao, X. Yan, F. Tang, and Q. Xue, "Enhancement in the fluorescence of graphene quantum dots by hydrazine hydrate reduction," Carbon **66**, 334–339 (2014).
29. L. Bao, Z. L. Zhang, Z. Q. Tian, L. Zhang, C. Liu, Y. Lin, B. Qi, and D. W. Pang, "Electrochemical tuning of luminescent carbon nanodots: from preparation to luminescence mechanism," Adv. Mater. **23**(48), 5801–5806 (2011).
30. L. Wang, S. J. Zhu, H. Y. Wang, S. N. Qu, Y. L. Zhang, J. H. Zhang, Q. D. Chen, H. L. Xu, W. Han, B. Yang, and H. B. Sun, "Common origin of green luminescence in carbon nanodots and graphene quantum dots," ACS Nano **8**(3), 2541–2547 (2014).

1. Introduction

Because of their unique optical properties, fluorescent nanoparticles have received intense scientific attention and are promising in bioapplications [1]. As a new emerging star in the field of fluorescent nanoparticles (NPs), carbon nanodots (C-dots) have drawn great attention since their initial discovery in 2004 because of their unique combination of intense photoluminescence (PL), high water solubility, chemical stability and photostability, low toxicity, and excellent biocompatibility [2, 3]. Thus, C-dots have broad application potential in biosensing [4, 5], bioimaging [6], drug delivery [7], and other optoelectronic applications [8, 9].

It is well known that Fe^{3+} is one of the most important ions in metabolic processes and is indispensable for all living systems because both deficiency and excess compared to the normal permissible level can induce serious disorders [10]. Therefore, the qualitative and quantitative determination of Fe^{3+} ions is essential in clinical, medical, and environmental applications. Recently, C-dots have been used for sensitive Fe^{3+} ion detection because of their excellent water solubility and low toxicity compared with previous organic chromophores and semiconductor quantum dots [4, 11]. However, most of the current synthesis methods, such as

#253046 Received 2 Nov 2015; revised 20 Dec 2015; accepted 21 Dec 2015; published 5 Jan 2016
© 2016 OSA

the chemical and thermal methods, involve toxic chemical reagents or complicated processes [12,13], which can be toxic and limit their application.

As a simple top-down approach, laser ablation in solution (LAS) is a "green" alternative to the conventional chemical routes, and the synthesis of C-dots in a well controlled, clean environment prevents any contaminations. In previous reports, however, the photoluminescent quantum yield (PLQY) of C-dots obtained by nanosecond LAS has been generally less than 10% [14, 15], which severely limits their availability for practical applications. Comparison with widely used nanosecond laser ablation, femtosecond laser ablation in solution (FLAS) synthesis of nanomaterials possesses unique properties. First, the energy of femtosecond laser is injected into the focus in an ultra-short time, a plasma plume with high temperature and high pressure is formed. The plasma temperature at focal point created by femtosecond laser, could be as high as 10^5 K [16], is much higher than that created by nanosecond laser (~10^3 K) [17]. Under these extreme conditions, the chemical reactions between the nanoclusters and the solution molecules are more drastic and NPs with abundant surface functional groups are formed. Second, the negligible heat effect of the femtosecond pulses also makes it possible to reduce the degradation of the solution, resulting in achievement of the desired low-toxic NPs for bioapplications [18]. In addition, the femtosecond laser can create much more extreme conditions, which are highly favorable for formation and stabilization of metastable phase nanocrystals such as nanodiamond and carbon related materials, cubic zirconia, etc [19, 20].

In this paper, using graphite powder as a carbon source, C-dots are prepared by femtosecond laser ablation in polyethylene glycol (PEG_{200N}) solutions with different graphite concentrations. The PL of the C-dots was effectively enhanced by decreasing the graphite concentration. The PLQY of the C-dots prepared with low concentration could reach 21% (excited at 290 nm), while the PLQY of the C-dots prepared with a high graphite concentration remained below 3%. To take advantage of their high photoluminescence properties, the C-dots were applied as very effective fluorescent nanosensor probes for sensitive and selective detection of Fe^{3+} ions.

2. Experimental

2.1 Synthesis of C-dots

In our previous report, C-dots with tunable emission have been synthesized using FLAS method with different laser parameters [21, 22]. Here, highly photoluminescent C-dots were synthesized by adjusting graphite concentrations. Typically, 0.5~5 mg of graphite powder, with a mean size of 400 nm, were dispersed into 50 ml of PEG_{200N} via ultrasonication. Next, ~10 ml of the suspension was put into a glass beaker for laser irradiation. The laser beam (Ti:sapphire femtosecond laser system, central wavelength: 800 nm, pulse duration: 150 fs, and repetition rate: 1 kHz) was focused on the suspension at a laser fluence of 150 J/cm^2 by a 25mm lens for about 30 min. During laser irradiation, a magnetic stirrer was used to prevent gravitational settling of the suspended powders. After laser irradiation, the solution was centrifuged, and the C-dots were obtained from the supernatant.

2.2 Characterization

Transmission electron microscopy (TEM) and high-resolution TEM (HRTEM) images of the C-dots were obtained via a high-resolution transmission electron microscope (model JEM-ARM200F). Through image analysis, the average diameter and size distribution were determined for ~1000 C-dots. X-ray diffraction (XRD) was performed with a PANalytical X-ray diffractometer. A U-3010 spectrophotometer (Hitachi) was employed to measure the absorption spectra of the samples. Fourier transform infrared spectroscopy (FTIR) was performed on a VERTEX 70 (Bruker) using the KBr pellet method. A small droplet of supernatant containing as-prepared C-dots was deposited on a KBr pellet and dried by placing the pellet in vacuum at 80°C for 6 h. The emission spectra measurements were performed on a FLS920 spectrometer (Edinburgh) with a bandwidth of 4 nm.

#253046 Received 2 Nov 2015; revised 20 Dec 2015; accepted 21 Dec 2015; published 5 Jan 2016
© 2016 OSA

2.3 Photoluminescent Quantum Yield (PLQY) measurements

The PLQY of the C-dots was measured using quinine sulfate (0.1 M H_2SO_4 as solvent; PLQY: 54%) as the standard and calculated with following equation:

$$QY_x = QY_{std} \frac{I_x}{I_{std}} \frac{A_{std}}{A_x} \frac{n_x^2}{n_{std}^2}$$

where *QY* is the quantum yield, *I* is the integrated emission intensity, *A* is the optical density, and *n* is the refractive index of the solvent. The subscripts "*std*" and "*x*" stand for standard with a known PLQY and the C-dot sample, respectively. In order to minimize reabsorption effects, the absorption value in a 10 mm fluorescence cuvette was kept below 0.10 at the excitation wavelength.

2.3 Detection of Fe^{3+} Ions

$FeCl_3$ was used to prepare Fe^{3+} with serial concentrations (0.1, 1, and 10 mM Fe^{3+}). The resulting Fe^{3+} solution was dropped into 2 ml of the C-dots solution (PEG_{200N}). After 3 min of ultrasonic dispersion, the change in fluorescence intensity was examined through a Hitachi F7000 spectrometer. Meanwhile, several metal ions (e.g., Na^+, Mg^{2+}, K^+, Ca^{2+}, Cu^{2+}, and Zn^{2+}) were employed to evaluate the selectivity.

3. Results and discussion

First, the structure and size distribution of as-prepared C-dots were analyzed by TEM and HRTEM images. Figures 1(a)-1(c) show the TEM images of C-dots prepared with graphite concentrations of (a) 12.5, (b) 50, and (c) 100 mg/L, respectively. The as-prepared C-dots distributed on the copper grid homogeneously, and no large aggregations could be observed, indicating that the C-dots were well dispersed in solution. The HRTEM images of C-dots prepared with concentrations of 12.5 and 50 mg/L (insets in Figs. 1(a) and 1(b)) exhibited highly crystalline structures with a lattice spacing of 0.21 nm, which is very close to the (100) in-plane lattice spacing of graphite [23]. The C-dots prepared with a higher concentration of raw material of 100 mg/L showed worse crystalline structure (insets in Fig. 1(c)).

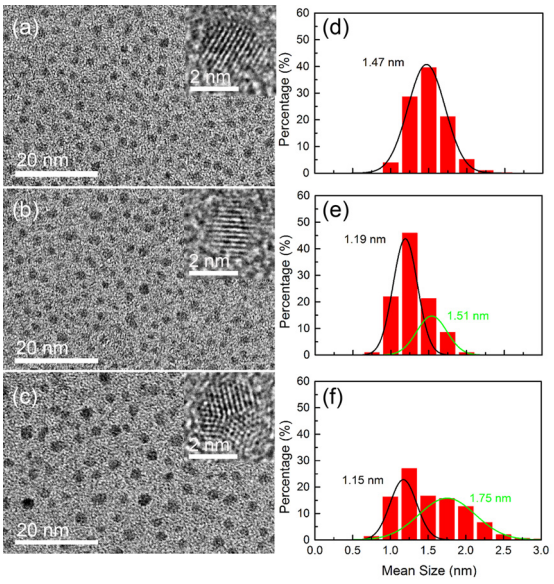

Fig. 1. TEM images of C-dots prepared by femtosecond laser ablation of graphite powder in PEG_{200N} with concentrations of (a) 12.5, (b) 50, and (c) 100 mg/L. The insets are the typical HRTEM images of the C-dots. (d, e, f) The corresponding size distributions of the C-dots presented in (a, b, c), respectively.

#253046 Received 2 Nov 2015; revised 20 Dec 2015; accepted 21 Dec 2015; published 5 Jan 2016
© 2016 OSA

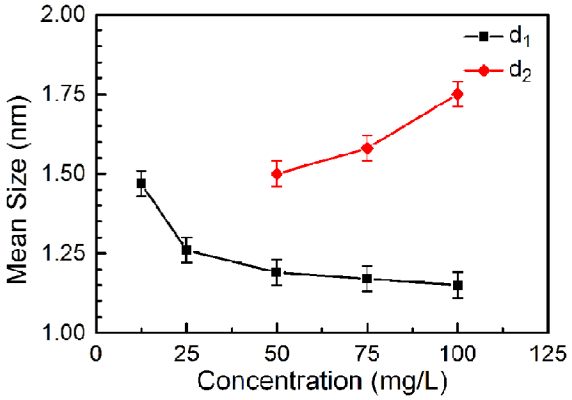

Fig. 2. Mean size for the small (d_1) and large (d_2) NPs of the as-prepared C-dots as a function of graphite concentration.

The size distributions of the corresponding products in Figs. 1(a)-1(c) are presented in Figs. 1(d)-1(f), respectively. For low concentrations (<50 mg/L), the size distribution could easily be fitted by a Gaussian function (Fig. 1(d)). However, for higher concentrations (≥50 mg/L), the single-peak Gaussian extrapolation was not adequate. An example of a distribution is shown in Fig. 1(f), in which most NPs are relatively small with a mean size of around 1 nm, but a significant number of large 1.5–3 nm NPs are still present. These distributions are well fitted by two Gaussian functions, suggesting that two different mechanisms might be involved in the production of NPs. The mean sizes of the small and large NPs as a function of graphite concentration are presented in Fig. 2. Figure 2 reveals that the mean size of small NPs progressively decreased with the graphite concentration, while that of large NPs began to appear and increased significantly when the graphite concentration varied from 50 to 100 mg/L. The results suggest that the large NPs gradually became dominant at high concentration, and the mean sizes of C-dots generally increased with the increase of graphite concentration, which is in agreement with results of a previous study on FLAS of Si NPs [24].

To confirm the lattice structures of the as-prepared C-dots, XRD patterns of the C-dots prepared with different graphite concentrations are shown in Fig. 3. The XRD patterns of C-dots prepared with graphite concentrations of 12.5 and 50 mg/L show distinct diffraction peaks in the range of 24.6–29.8° (Figs. 3(b) and 3(c)), which correspond to a graphitic structure [25]. The calculated *d* spacing between graphene layers ranged from 0.30 to 0.36 nm. In contrast, the XRD pattern of the C-dots prepared with a graphite concentration of 100 mg/L exhibits an amorphous structure with no obvious diffraction peak (Fig. 3(d)). The results further indicate that small C-dots prepared with a lower graphite concentration have a higher crystalline structure compared with large C-dots prepared with a higher concentration.

Here, we give a brief interpretation of the possible mechanisms of effects of source concentration on size distributions and structures of C-dots in FLAS. As suggested by several researchers, when the femtosecond pulses inject into the solid targets, Coulomb explosion occurs, and a plasma plume with high temperature and high pressure forms because of multiphoton absorption ionization [16, 18]. When the plasma plume expands and cools down, a cavitation bubble is generated in solution [17]. With the expansion of the bubble, carbon nanoclusters with high surface energy in the cavitation bubble tend to aggregate into larger NPs [26, 27]. When the temperature decreases and the internal pressure of the bubble drops to a value lower than that of the surrounding solution, C-dots with reduced size are formed. Recently, we found that an increase in the laser fluence increased the bubble temperature and pressure, and as a result, larger C-dots were produced [21].

#253046 Received 2 Nov 2015; revised 20 Dec 2015; accepted 21 Dec 2015; published 5 Jan 2016
© 2016 OSA

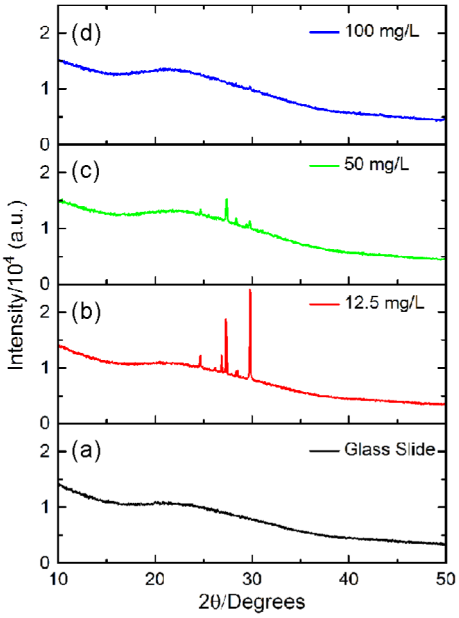

Fig. 3. XRD patterns of C-dots prepared by femtosecond laser ablation of graphite with different concentrations.

In this work, the focus spot size (~4 μm) was much larger than the size of the initial graphite powders (<400 nm). Thus, many initial graphite powders may be ablated simultaneously, and C-dots are produced in independent cavitation bubbles or in large bubbles merged from many bubbles during their expansion. We suggest that the highly crystalline, small C-dots prepared with low graphite concentration were likely produced in independent cavitation bubbles, in which most of the C-dots originated from the nanoclusters produced in the initial stage of cavitation with high temperature and pressure. In this case, the laser energy in the focused zone is expected to decrease with increase the graphite powder concentration, because a fraction of the laser energy is absorbed by suspended graphite powders above the focused point. As a result, the temperature and pressure of the bubble decrease, resulting in the gradual decrease in the size of C-dots. However, many adjacent cavitation bubbles with different temperatures and pressures might merge into a large bubble during their expansion with a further increase in graphite concentration. The nanoclusters with higher concentration further aggregate into larger NPs that have worse crystalline structure (Fig. 4). These large C-dots are dominant, and their mean size gradually increases with the graphite concentration.

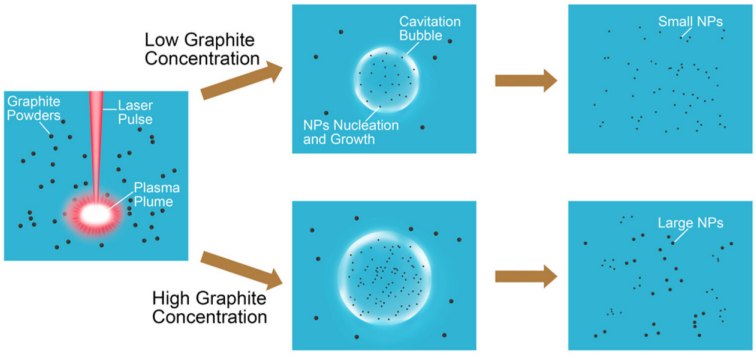

Fig. 4. Schematic illustration of FLAS of graphite powder with different concentrations.

#253046 Received 2 Nov 2015; revised 20 Dec 2015; accepted 21 Dec 2015; published 5 Jan 2016
© 2016 OSA

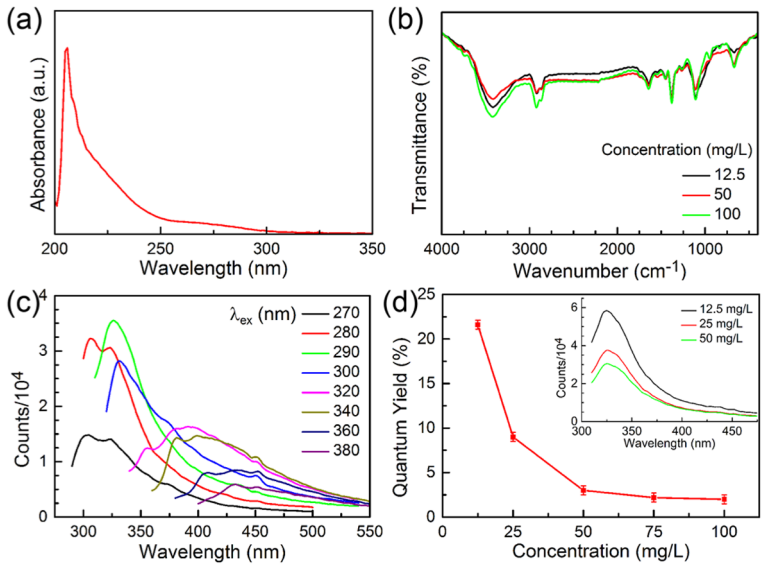

Fig. 5. (a) A typical UV-Vis absorption spectrum of the C-dots. (b) FTIR spectra of the C-dots prepared with different concentrations. (c) A typical steady-state PL spectra of the as-prepared C-dots in PEG_{200N} solution. (d) The PLQY of as-prepared C-dots as a function of graphite concentration. The inset is the emisison spectra of different C-dots at 290 nm excitation.

To study the effect of graphite concentration on PL properties, we explored the UV-Vis absorption spectra and FTIR spectra of the C-dots. The UV-Vis absorption spectra of all C-dots showed absorption peaks at 205 nm, which are attributed to the π-π* transition of the C = C double bond in the carbogenic core (Fig. 5(a)) [28]. Analysis of the FTIR spectra of C-dots prepared with different graphite concentrations showed that the surface functional groups in these C-dots were similar (Fig. 5(b)). For example, there are stretching vibrations of the O-H bond at 3420 cm^{-1} [23], the C-H bond at 2920 cm^{-1} and 2855 cm^{-1} [19], the C = O double bond at 1630 cm^{-1} [23], and the C-O bond around 1000–1200 cm^{-1} [19].

Although different in size, C-dots prepared with different graphite concentrations exhibited similar PL properties. The emissions of as-prepared C-dots were mainly in the UV region with a maximum intensity around 325 nm (excited at 290 nm) (Fig. 5(c)). The PLQY of the C-dots at 290 nm excitation was measured. The PLQY of C-dots prepared with concentrations of 12.5, 50, and 100 mg/L were estimated to be 21.6, 3.0, and 2.1%, respectively. The PLQY of C-dots as a function of graphite concentration revealed that the PLQY increased sharply with decreasing graphite concentration (Fig. 5(d)). Its values were below 3% when graphite concentrations were larger than 50 mg/L. The results indicate that C-dots prepared at lower carbon concentrations exhibited stronger PL emission.

Some luminescence mechanisms of C-dots have been suggested, such as quantum-confinement effects, emissive traps, electronic conjugate structures, etc [29]. Recent reports suggested that drastic competition among different emission centers (special structures consisting of edge carbon atoms and functional groups) and traps (meaningless structures, defects) dominate the optical properties of C-dots. Hence, more unitary functional group with larger quantity created on a highly crystalline carbongenic core will result in higher PLQY. In contrast, lower PLQY can be observed for C-dots with more traps and fewer surface functional groups [30]. In this study, highly crystalline carbongenic cores of C-dots prepared at low concentrations contained fewer trap defects. Furthermore, with the decrease in the graphite concentration, the chemical reactions between the nanoclusters and the solution molecules were more drastic because of the higher temperature of the plasma plume. Consequently, more surface functional groups might be created. Thus, a decrease in carbon source concentration in FLAS leads to an increase in PLQY.

#253046 Received 2 Nov 2015; revised 20 Dec 2015; accepted 21 Dec 2015; published 5 Jan 2016
© 2016 OSA

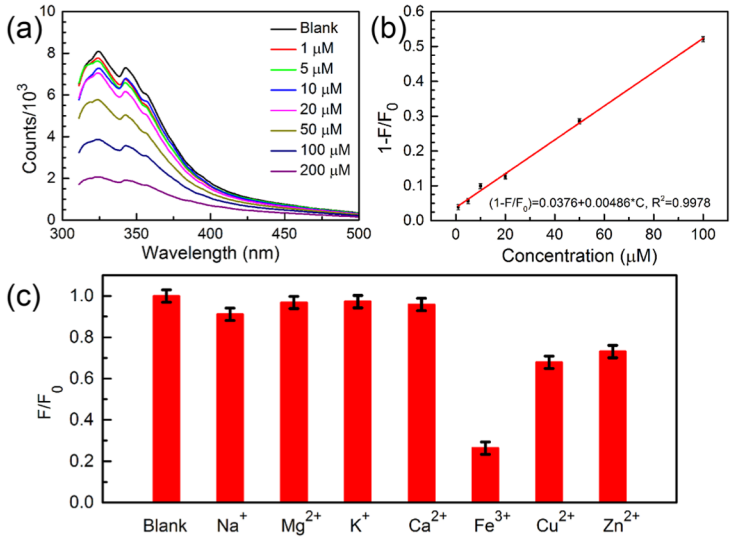

Fig. 6. (a) Emission spectra of C-dot solutions with different concentrations of Fe^{3+} ions (0–200 μM) at 290 nm excitation. (b) The dependence of 1-(F/F_0) on the concentration (0–100 μM) of Fe^{3+} in PEG_{200N} solution. (c) Comparison of fluorescence intensities at 325 nm of C-dots in the presence of various metal ions (200 μM for Na^+, Mg^{2+}, K^+, Ca^{2+}, Fe^{3+}, Cu^{2+}, and Zn^{2+} in 2 ml of C-dot solution). F_0 and F stand for the fluorescence intensities at 325 nm in the absence and presence of metal ions, respectively.

By taking advantage of their superior purity compared to their chemically synthesized counterparts and their high PL properties, various new applications of C-dots can be anticipated. Here, as an example for bioapplications, the C-dots prepared with a graphite concentration of 12.5 mg/L were utilized in a sensing application for the highly sensitive and selective detection of Fe^{3+} ions. As shown in Fig. 6(a), the fluorescence intensity of C-dots gradually decreased from ~8100 to 2000 (a.u.) with an increase in the concentration of Fe^{3+} ions from 1 to 200 μM (in PEG_{200N} solution). We used 1-F/F_0 as an indicator for the detection of Fe^{3+}, where F_0 and F present the fluorescence intensity of the C-dot solution in the absence and presence of Fe^{3+} ions, respectively. A good linear correlation was obtained over a concentration of Fe^{3+} ions ranging from 1 to 100μM with a correlation coefficient of 0.9978 (Fig. 6(b)). To evaluate the selectivity of the proposed Fe^{3+} sensor, we examined the fluorescence intensity ratio F/F_0 in the presence of various metal ions, including Na^+, Mg^{2+}, K^+, Ca^{2+}, Cu^{2+}, and Zn^{2+}. As shown in Fig. 6(c), Fe^{3+} ions had the greatest effect on fluorescence quenching among the metal ions tested. The fluorescence quenching by Fe^{3+} ions is ascribed to nonradiative electron transfer involving partial transfer of an electron in excited state to the *d* orbital of Fe^{3+}. For Cu^{2+} and Zn^{2+} ions, the slight fluorescence quenching can be attributed to the nonspecific interactions between the carbonxilic groups and the metal ions [4, 11]. Although exist the interference of Cu^{2+} and Zn^{2+} ions, the effects is slighter and the selectivity of Fe^{3+} detection is higher than others reports [4, 11].

4. Conclusion

In conclusion, we have introduced a simple strategy to enhance the PL of C-dots prepared by FLAS. The PLQY of the C-dots increased sharply with decreasing graphite concentration, and the value could reach 21% (excited at 290 nm). Detailed work showed that the C-dots prepared at low carbon concentration possessed high PLQY due to fewer trap defects in the carbogenic core and a large quantity of surface functional groups. Our experiments further demonstrated that the C-dots prepared by LAS are promising for bioapplications. Here, as an example, high PL C-dots were applied as very effective fluorescent nanosensor probes for sensitive and selective detection of Fe^{3+} ions.

#253046 Received 2 Nov 2015; revised 20 Dec 2015; accepted 21 Dec 2015; published 5 Jan 2016
© 2016 OSA

Acknowledgments

This work was supported the by the National Basic Research Program of China (973 Program) under Grant No. 2012CB921804, the National Natural Science Foundation of China (Grant No. 61235003, 11304242 and 11474078), the Natural Science Basic Research Plan in Shaanxi Province of China (Program No. 2014JQ1024), the Financial Grant from the China Postdoctoral Science Foundation (Grant No. 2013M542335 and 2014T70924), and the collaborative Innovation Center of Suzhou Nano Science and Technology. The TEM work was performed at the International Center for Dielectric Research (ICDR), Xi'an Jiaotong University, Xi'an, China. The authors also thank Mr. Ma and Ms. Lu for their help with TEM.

#253046 Received 2 Nov 2015; revised 20 Dec 2015; accepted 21 Dec 2015; published 5 Jan 2016
© 2016 OSA